

## Regional Aircraft Measurement of CO<sub>2</sub>

### - Study on Natural Sinks and Sources of CO<sub>2</sub> in Iriomote Island in Japan -

Susumu YAMAMOTO, Hiroaki KONDO, Minoru GAMO,  
Naoki KANEYASU and Masayasu HAYASHI

( Environmental Assessment Dept., National Institute for  
Resources and Environment, Onogawa, Tsukuba, Ibaraki 305,  
Japan )

Mitsunori ARAMOTO

( College of Agriculture, University of the Ryukyus,  
Okinawa 903-01, Japan )

#### Abstract

In this study, field observations using an airplane, two boats and a tower were carried out above and around Iriomote Island in Okinawa Prefecture ( 123.9° E, 24.2° N ) to study the behavior of CO<sub>2</sub> under subtropical conditions and to estimate the exchange rates of CO<sub>2</sub> between the atmosphere and the sea or vegetation.

We carried out field measurement over the Iriomote from 21th to 24th of March, 1991. In this measurement, the spatial and time variations of the CO<sub>2</sub> concentration and meteorological conditions were measured by an airplane and a tower. The air above and around the Iriomote was sampled using an airplane and two boats. The concentration of CO<sub>2</sub> was analyzed by a non-dispersive infrared gas analyzer.

According to observational results, CO<sub>2</sub> concentration in down-wind side is smaller than the value in up-wind side by 1ppm at the height of 400m and by 2 ppm at 200 m. These results indicate the intake of CO<sub>2</sub> due to the photosynthesis of vegetation in the Iriomote.

The decrease of CO<sub>2</sub> due to activity of vegetation was calculated using the plume diffusion model with Pasquill diffusion parameters. In the diffusion model, the negative sources, -2 g/(m<sup>2</sup>hr) was assumed for the value of net-intake rate of CO<sub>2</sub> as the result of vegetation activities including photosynthesis, respiration and decay of organic matter.

The results of diffusion calculation compared with the differences between CO<sub>2</sub> concentrations observed in the down-wind side and up-wind side. From above comparison, we can get a value of 2 to 3 g/(m<sup>2</sup>hr) for intake rate of CO<sub>2</sub> due to the activity of vegetation under the daytime condition of the Iriomote in March.

## 1. Introduction

The assessments of CO<sub>2</sub> concentration in the future and its impact on environment have large ambiguity due to the uncertain behavior of CO<sub>2</sub> in the environment and uncertainty of the fossil-fuel consumption.

In this study, field observations using an airplane, two boats and a tower were carried out above and around Iriomote Island in Okinawa Prefecture ( 123.9° E, 24.2° N ) to study the behavior of CO<sub>2</sub> under subtropical conditions and to estimate the exchange rates of CO<sub>2</sub> between the atmosphere and the sea or vegetation.

About 90% of Iriomote Island is covered with the sub-tropical forest and artificial sources of CO<sub>2</sub> are few. Therefore, the Iriomote is a suitable site to investigate the role of sub-tropical forest in the budget of CO<sub>2</sub>.

We carried out field measurement over the Iriomote from 21th to 24th of March, 1991. In these measurements, the spatial and time variations of the CO<sub>2</sub> concentration and meteorological conditions such as air-temperature, wind and insolation were measured by an airplane and a tower. The air around and over the Iriomote was sampled using an airplane and two boats. The concentration of CO<sub>2</sub> was analyzed by a non-dispersive infrared gas analyzer.

In the same period, National Institute for Environmental Studies measured the concentration of the hydro-carbon compounds above and around the Iriomote. The observational base of the Iriomote was set at the Center for Tropical Agriculture belonging to University of Ryukyus, Ishigaki airport was used as the base of airplane measurement.

In this paper, mainly, the results of CO<sub>2</sub> measurement by airplane are mentioned.

## 2. Outline of Measurements

Spatial observations of CO<sub>2</sub> concentration, temperature and

humidity were made by a light airplane, Cessna - 404 from 21th to 24th of March, 1991. Flight times and conditions are listed in Table 1. Total number of flights was 8 runs and the flight path covered two or three heights between 200m and 1000m and the duration of each run was approximately one and half hours. Flight speed was about 150 knots.

TABLE 1. Observation dates and flight heights.

Run	Date	Flight heights and courses
IRIOMOTE MAR-1991-1	March 21 9:29-11:16	Ascending (take-off) flight:0-3000ft Constant :2060,1360,665ft/Rectangular level flight flight over sea
IRIOMOTE MAR-1991-2	March 21 12:38-13:39	Ascending:0-3000ft Constant:1350,670ft/Rectangular over sea
IRIOMOTE MAR-1991-3	March 21 15:28-16:52	Ascending:0-3000ft Constant:1360,665ft/Rectangular over sea
IRIOMOTE MAR-1991-4	March 23 9:37-10:44	Ascending:0-3000ft Constant:1020,500ft/Rectangular over sea
IRIOMOTE MAR-1991-5	March 23 12:28-13:33	Ascending:0-3000ft Constant:1020,505ft/Rectangular over sea
IRIOMOTE MAR-1991-6	March 23 15:27-16:47	Ascending:0-1500ft Constant:1315,655ft/Flight over south-western sea
IRIOMOTE MAR-1991-7	March 24 9:25-11:01	Ascending:0-3000ft Constant:2060,1330,670ft/Flight over northern and southern sea Constant:2060ft/Flight over the island
IRIOMOTE MAR-1991-8	March 24 12:18-13:25	Ascending:0-3000ft Constant:2040,1340,665ft/Flight over western sea Constant:1650ft/Flight over the island

The topographical condition of the Iriomote is mountainous with several peaks about 400 m in height are situated at the central part of the island and north and south coastal areas. Fig.1 is a map of the observation site including the air sampling points of ; S1 - S3, the measurement tower;T and wind observation points using pilot balloon; P1,P2.

The flight courses were chosen for the purpose of measurement from among rectangular flight (20km x 4 legs), crossing flight ( 20-30km ) over the Iriomote and long distance flight ( 30-40km ) in the down-wind side of the island.

Weather conditions during observation days were as follows;  
[ March 21 ]

The observation site was covered with clouds of base height between 700m and 1000m. But, there were some intervals of clear weather with no precipitation. The wind direction was between

S and SSE with a speed of 3-4 m/s at the surface.

[ March 22 ]

The front passed over the Iriomote from north to south in the afternoon of March 22, weather condition became unstable and the base height of clouds was lower than 500m. The weather deteriorated further and there was a shower in the evening. The wind direction was NE and its speed was 5-6 m/s at the surface.

[ March 23 ]

The sky was almost totally covered with cloud, but the height of cloud base was above 1000m with some intervals of clear weather. The wind was weak ( 2 - 3 m/s ) and its direction fluctuated between S and E.

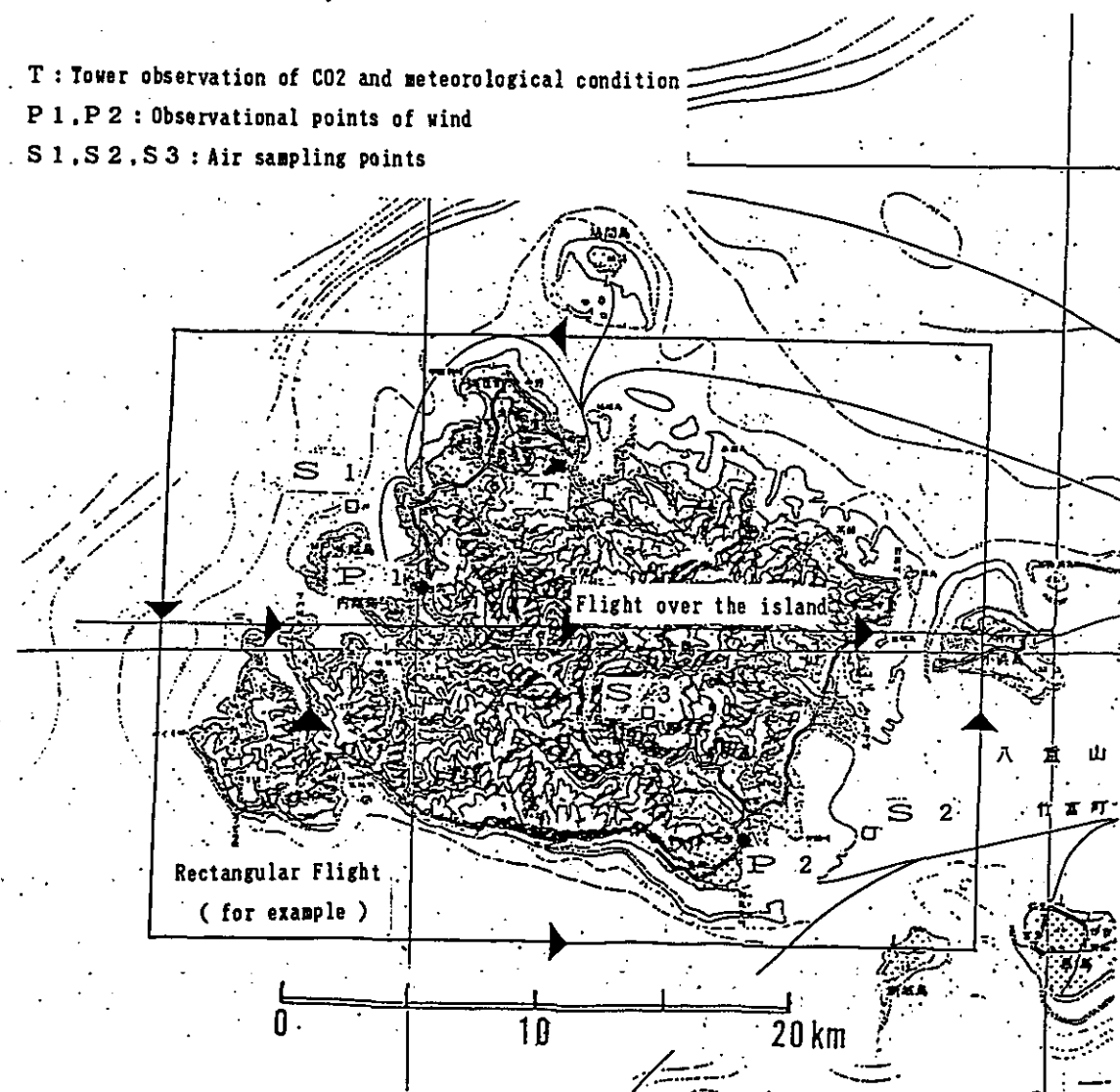


FIGURE 1. Map of the observation site ( Iriomote Island ).

### 3. Instrumentations and analysis

An infrared CO<sub>2</sub> sensor with open sensing path was installed in the cabin. Outside air was introduced to the sensor through a pipe. A dry and wet bulb thermistor-thermometer was used to measure the mean temperature and mean humidity, and mixing ratio of water vapor was measured by a Lyman-alpha hygrometer. Flight altitude was estimated from the output of a barometer. Two or three air samples were taken at each flight level and CO<sub>2</sub> concentration was determined by a non-dispersive infrared analyzer in the laboratory.

#### 3.1 Infrared CO<sub>2</sub> sensor for continuous measurement by airplane

Fast response sensor and rigid instrument of anti-vibration type are needed to measure CO<sub>2</sub> from an airplane. In this experiment, we used a CO<sub>2</sub> sensor developed by Advanced System Corp., Japan. The concentration of CO<sub>2</sub> is measured using the absorption band of 4.3  $\mu\text{m}$  infrared radiation. Relative error and response frequency of this sensor are less than 0.5 ppm and higher than 10 Hz, respectively. This sensor is vibration resistant, but it has drift-error of zero level due to temperature changes of environment.

The diagram of the sensor is shown in Fig.2. Infrared radiation emitted from the heater is collimated by the CaF<sub>2</sub> lens. Through the sensing path ( 20cm in length ), the beam is focused at the detector part by the other CaF<sub>2</sub> lens. And it reaches to the infrared detector through a filter. Infrared radiation beam is chopped by a rotating disk equipped with two filters for measuring and the reference wavelengths. The concentration of CO<sub>2</sub> is calculated from the ratio of the strengths of measuring and reference beams.

We had a plan to install the CO<sub>2</sub> sensor on the nose-boom of the airplane to measure the fluctuations of CO<sub>2</sub> concentration

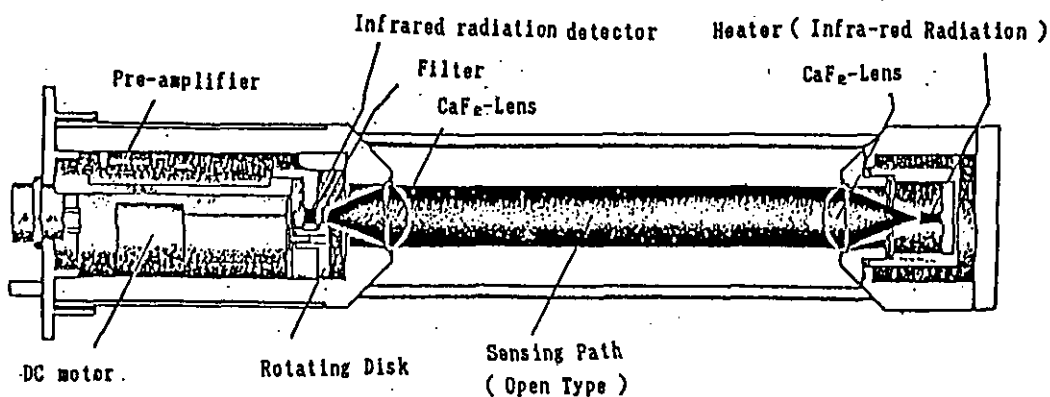


FIGURE 2. Diagram of the infrared CO<sub>2</sub> sensor( open-path type ).

directly. But, the present type sensor is not strong enough to be installed outside the airplane. Then, in this experiment, the sensor was set in the cabin of airplane. The sensing path was covered by a cylindrical tube, and outside air was introduced into the sensing path through the cylinder. The sensitivity of this sensor is affected by temperature and the zero-level of output changes with time. We calibrated the sensor using standard CO<sub>2</sub> gas of two concentrations before and after the measurements at each flight level. The output of the sensor is approximately proportional to air pressure, so the error of CO<sub>2</sub> fluctuations due to pressure (height) change was corrected according to this assumption.

### 3.2 Air sampling and its analysis

Surface air samples were taken at the three points including two onboard ship and one point at an inner site on the Iriomote. The upper atmosphere around and above the Iriomote were sampled by the airplane. The frequency of sampling by airplane was 2 or 3 times at each flight level and 6 to 9 samples were taken during one run.

Air sample containers are cylindrical stainless-steel flasks with one liter capacity each. Before sampling, the flasks are evacuated to remove contaminants. The air samples are pressurized up to about 3 atm using an electric diaphragm pump.

These air samples were analyzed by a non-dispersive infrared CO<sub>2</sub> analyzer manufactured by Hitachi-Horiba Co., Japan. Since the NDIR gas analyzer is for relative measurement, it requires standard gases defined by the CO<sub>2</sub> absolute calibration system. System of CO<sub>2</sub> analysis and calibration follow the method developed by Tanaka et al. (1983). We used four standard gases between 321 ppm and 411 ppm of CO<sub>2</sub>-based pure air for calibration. A precision of better than 0.1 ppm was attained.

This type of analyzer is heavy and weak against vibration. Therefore, we cannot use it for the airplane sensor.

### 4. Observational results

Fig.3 is one example of CO<sub>2</sub> concentration measured by airplane ( 9:47-11:07, March 21 ). The flight path takes a rectangular pattern around the Iriomote. In this example, wind direction is between S and SSW, so flight legs of southern and northern part of the island correspond to up-wind and down-wind side, respectively. The flight legs were taken at 3 levels; 2060, 1360, 665 ft ( 600, 400, 200 m ). According to results, CO<sub>2</sub> concentration in up-wind side decreases with height, and it is nearly constant with height in down-wind side. Furthermore, its concentration in down-wind side is smaller than the

value in up-wind side by 1ppm at the height of 400m and by 2 ppm at 200 m. These results indicate the mixing of atmosphere due to the topographical effect of the Iriomote and the intake of CO<sub>2</sub> due to the photosynthesis of vegetation in the Iriomote.

Fig.4 shows two examples of CO<sub>2</sub> concentration measured by the crossing flights over the Iriomote. The upper graph in Fig.4 is the case of a crossing flight from A' to B' at the height of 600m (10:14-18, March 24). The wind direction in this case is easterly and depression of CO<sub>2</sub> concentration is about 3 ppm over the center of the island. The lower graph in Fig.4 is the case of a

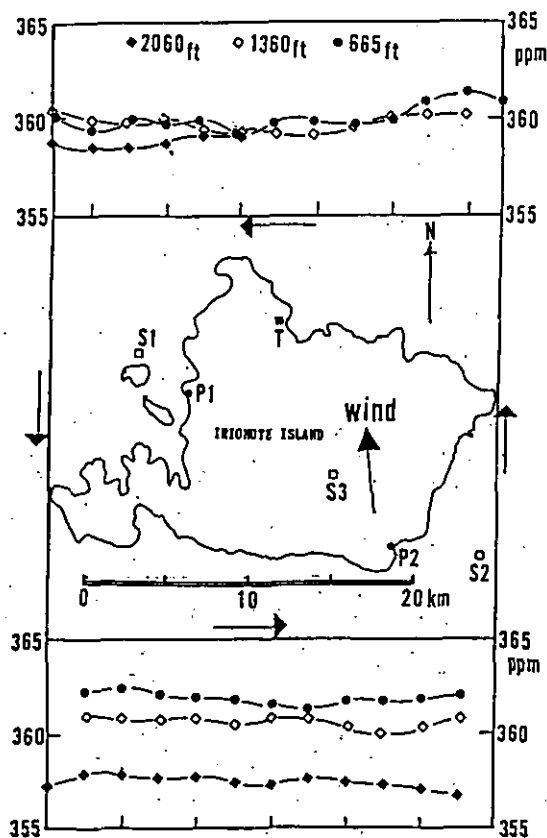


FIGURE 3. One example of airplane measurement of CO<sub>2</sub> concentration around the Iriomote (IRIOMOTE-MAR-1991-1, 3/21 9:47-11:07, heights: 2060, 1360, 665 ft (600, 400, 200m)).

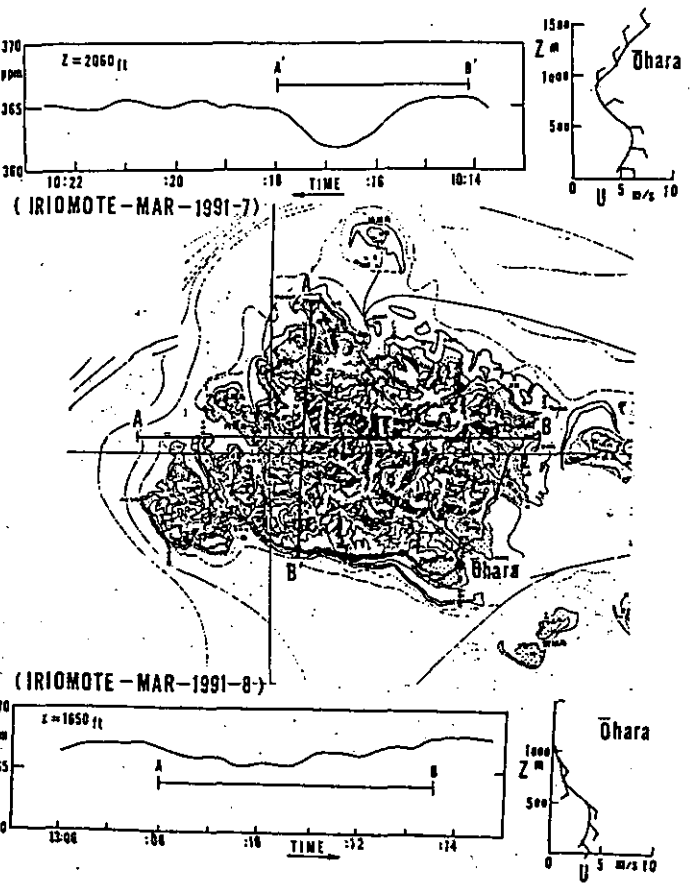


FIGURE 4. Airplane measurements of CO<sub>2</sub> concentration above the Iriomote (IRIOMOTE-MAR-1991-7, 3/24 10:14-10:18, height: 2060ft (600m), A'-B' and IRIOMOTE-MAR-1991-8, 3/24 13:08-13:14, height: 1650ft (500m), A-B).

crossing flight from A to B at 400 m (13:08-14, March 24). The wind direction in this case is SE and CO<sub>2</sub> depression is about 2 ppm over the center of the island.

## 5. Discussion of the results

We chose the Iriomote for the experiment site by the reasons that the subtropical forest is distributed uniformly in the island and the artificial emission of CO<sub>2</sub> is small. However, the area is too large to clarify the CO<sub>2</sub> distribution all over the island only by the experiment. Then, the decrease of CO<sub>2</sub> due to activity of vegetation was calculated using the plume diffusion model with Pasquill diffusion parameters.

In the diffusion model, the negative sources (intake of CO<sub>2</sub> by vegetation) were given at the every mesh (1 km x 1 km, area sources) over the island, and the source height was 2m above the ground surface. The ground level above sea surface was taken from the topographical data, but the mechanical effects of topography were not considered. The source intensity, -2 g/(m<sup>2</sup>hr) was assumed for the value of net-intake rate of CO<sub>2</sub> as the result of vegetation activities including photosynthesis, respiration and decay of organic matter. In actual condition, intake value of CO<sub>2</sub> by vegetation depends on species of plants, meteorological condition and CO<sub>2</sub> concentration, but we use this as mean and representative value of net CO<sub>2</sub> intake due to the activity of subtropical vegetation during clear daytime in March.

Fig.5 shows the result of diffusion calculation model with the diffusion condition at the time of measurement indicated in Fig.3; U=5m/s, wind direction=S, Pasquill atmospheric stability=C). This graph is a horizontal distribution of CO<sub>2</sub> decrease from the concentration in the up-wind side. From this result, the decrease of CO<sub>2</sub> concentration is about 2ppm over the north coast of the island and from 1 to 1.5 ppm over the northern sea of the island in down-wind side.

Fig. 6 is a comparison between vertical profile of decrease of CO<sub>2</sub> calculated by diffusion model and vertical profile of CO<sub>2</sub> concentration observed by airplane at the three heights; 200, 400 and 600m. The decreases of CO<sub>2</sub> in calculation are about 2 ppm at the height of 200m and 1.5 ppm at 400m. This result is consistent with the differences between CO<sub>2</sub> concentrations observed in the down-wind side and up-wind side. This result indicates that the intake rate of CO<sub>2</sub>, 2 g/(m<sup>2</sup>hr) used in the calculation is appropriate.

Fig.7 shows the result of diffusion calculation using the diffusion condition at the time of the measurement of Fig.4; U=3

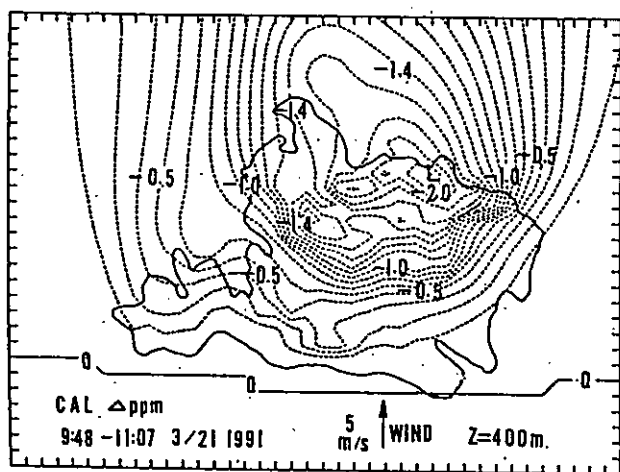


FIGURE 5. Horizontal distribution of CO<sub>2</sub> concentration decrease calculated by Pasquill diffusion model ( height=400m, wind=5m/s, S, stability=C ).

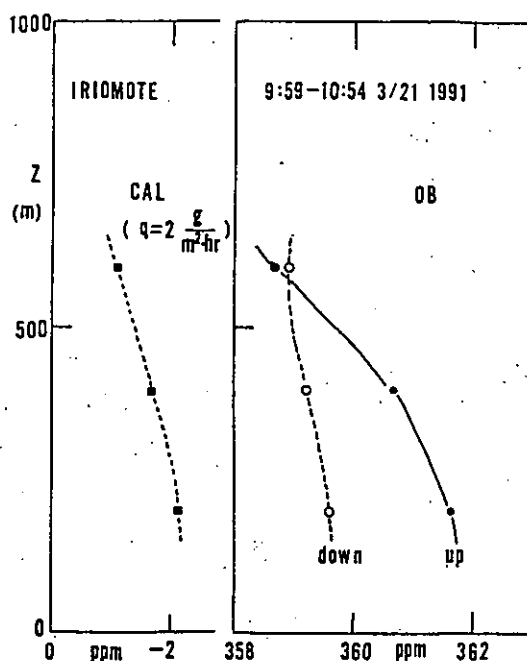


FIGURE 6. Comparison of the vertical profiles of CO<sub>2</sub> concentration decrease according to the diffusion calculation ( FIG.5 ) with airplane measurement of CO<sub>2</sub> ( FIG.3 ) in the down-wind and up-wind sides of the island.

m/s, wind direction=SE, stability=C. The decrease due to the CO<sub>2</sub> intake of vegetation is more than 2 ppm at the center of the island according to this result.

Fig.8 is a comparison between horizontal distribution of decrease of CO<sub>2</sub> according to the calculation ( Fig.7 ) and the horizontal variation of CO<sub>2</sub> concentration observed by airplane ( lower graph of Fig.4 ). In this calculation, the value, 2 g/(m<sup>2</sup>hr) was used for the net-intake rate of CO<sub>2</sub>, but the value, 2.5 g/(m<sup>2</sup>hr) is more agreeable to the observed result.

## 6. Conclusions

From above discussion, we can get a value of 2 to 3 g/(m<sup>2</sup>hr) for intake rate of CO<sub>2</sub> due to the activity of vegetation under the daytime condition of the Iriomote in March. From the product of this value by whole area of the Iriomote ( 20,000 ha ), we can

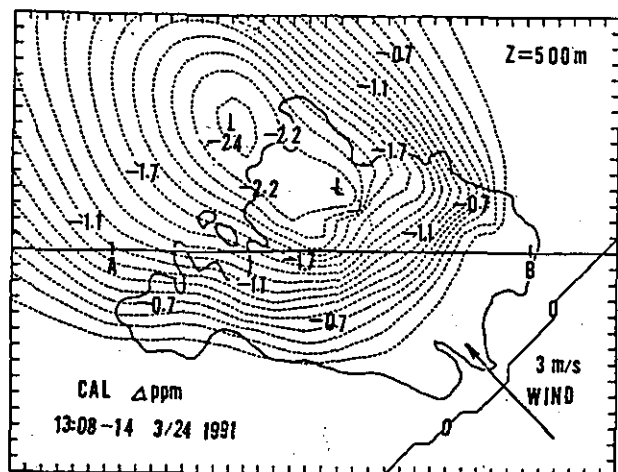


FIGURE 7. Horizontal pattern of CO<sub>2</sub> concentration decrease calculated by Pasquill diffusion model (height=500m, wind=3m/s,SE, stability=C).

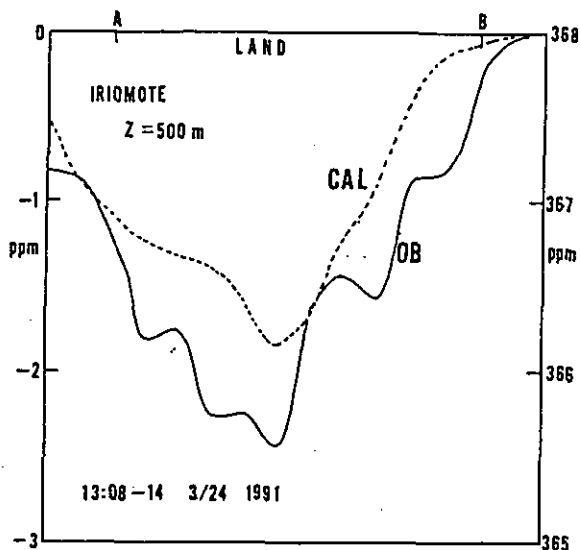


FIGURE 8. Comparison of the horizontal distribution of CO<sub>2</sub> concentration decrease according to the diffusion calculation ( FIG.7 ) with airplane measurement of CO<sub>2</sub> concentration ( FIG.4 ).

estimate that the total intake of CO<sub>2</sub> due to the vegetation in the Iriomote is between 400 to 600 tons/hr. However, this is a value for clear daytime in spring. When we estimate the net intake of CO<sub>2</sub> during the whole year, we should consider the intake or emission of CO<sub>2</sub> under the conditions of night time and non-active seasons such as autumn and winter. We would like to carry out more field experiments and to investigate the net-intake of CO<sub>2</sub> in such conditions.

Because the strength of the CO<sub>2</sub> sensor is not enough, we cannot measure CO<sub>2</sub> fluctuations using the sensor installed outside the airplane. Therefore, in this study, we cannot calculate the CO<sub>2</sub> flux directly using the fluctuation data of CO<sub>2</sub> concentration and wind speed observed by airplane. Calculation of the CO<sub>2</sub> flux using the eddy correlation method may be necessary to clarify fine mechanism of CO<sub>2</sub> exchange between the atmosphere and vegetation or the sea. This problem has to be investigated as a next step.

## References

1. M.Tanaka,T.Nakazawa and S.Aoki,"High Quality Measurements of the Concentration of Atmospheric Carbon Dioxide",J. of Meteorological Soc. of Japan,61:678-685 (1983).
2. S.Yamamoto,M.Gamo and O.Yokoyama,"Aircraft Observation of the Specific Humidity and Process of the Water Vapor Transfer in the Upper Mixed Boundary Layer",J. of Meteorological Soc. of Japan,66:141-154 (1988).
3. E.Ohtaki,T.Seo and T.Matsui,"Development of Fast Response Carbon Dioxide Instrument", Tenki, 34(5):3-14 (1987) (in Japanese).
4. S.Yamamoto,H.Kondo,M.gamo,et al., "Study on the Natural Sinks and Sources of CO<sub>2</sub> in Iriomote Island, (2) Airplane Measurement of CO<sub>2</sub> Concentration", Kogai, 27(1):73-82 (1992) (in Japanese).

Role of Intertropical Convergence Zone and South Pacific Convergence Zone  
for the Transport of Various Trace Gases from the Northern Hemisphere to the  
Southern Hemisphere.

Takakiyo Nakazawa  
Center for Atmospheric and Oceanic Studies  
Tohoku University, Sendai 980, Japan

In 1982, we began systematic collection of air samples on board a commercial container ship sailing between Yokohama, Japan and Melbourne, Australia, to elucidate spatial and temporal variations of the lower tropospheric CO<sub>2</sub> concentration over an extensive geographical area. Approximate cruise tracks are shown in Fig. 1. As seen in Fig. 2, we found from this measurement that the CO<sub>2</sub> concentration changes discontinuously at southern low latitudes for the period from December to May when the CO<sub>2</sub> concentration at low latitudes is higher in the northern hemisphere than in the southern hemisphere. A similar phenomenon is found in the distribution of the atmospheric CH<sub>4</sub> concentration, as seen in Fig. 3. Ship-board measurements were also made in the eastern part of the Pacific Ocean from 1984 to 1986, using two commercial container ships sailing between Tokyo and New York, U.S.A., to examine the longitudinally different variations of the lower tropospheric CO<sub>2</sub> concentration. From this measurement, discontinuous change of the CO<sub>2</sub> concentration was observed at northern low latitudes, especially in winter and spring, as shown in Fig. 4. The South Pacific Convergence Zone (SPCZ) is usually located at latitudes between 5° and 10°S on the cruise track of our ship in the western part of the Pacific Ocean, and the Intertropical Convergence Zone (ITCZ) is situated, on average, at 5°N in the eastern part of the Pacific Ocean and moves northward and southward with season. Since rapid air exchange between the northern and southern hemispheres is hindered by the ITCZ and SPCZ, discontinuous change of the concentration can be attributed to the suppression of southward transport of the northern hemispheric air with rich CO<sub>2</sub> and CH<sub>4</sub> due to existence of these convergence zones. The ITCZ and SPCZ disappear in Southeast Asia during the period from June to November, due to the monsoon circulation, and the southern hemispheric air intrudes into the northern hemisphere through the lower troposphere. Therefore, the southward transport of various trace gases originated in the northern hemisphere across these convergence zones through the lower troposphere may not be so effective for their increase in the southern hemisphere.

To elucidate variations of the upper tropospheric CO<sub>2</sub> concentration, we made aircraft measurements between Tokyo and Sydney, Australia and between Tokyo and Anchorage, Alaska in 1984 and 1985. Figure 5 shows average values of yearly mean CO<sub>2</sub> concentrations of 1984 and 1985 in the lower and upper troposphere and at 7.2 km height over Anchorage and Sydney. The lower tropospheric values were obtained mainly from our other programs, but the results of continuous measurements at two CMDL stations of Pt. Barrow, Alaska and the South Pole are also included in this figure. Values are represented as a deviation from the South Pole. The concentration of the lower tropospheric CO<sub>2</sub> is high at mid- and high northern latitudes and decreases southward. On the other hand, the concentration of the upper tropospheric CO<sub>2</sub> is high in the equatorial region centered at 5°N and decreases gradually poleward. Upward transport of the lower tropospheric air near the ITCZ may be responsible for this distribution. As described before, the ITCZ is usually located at 5°N on the Pacific Ocean to the windward of our flight routes. In the northern hemisphere, lower tropospheric values are higher than upper tropospheric values, reflecting the fact that a large amount of CO<sub>2</sub> is released into the atmosphere by fossil fuel combustion, and the situation is reversed in the southern hemisphere. The vertical CO<sub>2</sub> profile in the southern hemisphere is attributed to southward transport of the northern hemispheric air through the upper troposphere, as will be discussed later, and to the CO<sub>2</sub> uptake by the southern hemispheric oceans.

Figure 6 shows the seasonal CO<sub>2</sub> cycles in the upper troposphere at respective latitudes and at 7.2 km height over Anchorage and Sydney. One division of the ordinate corresponds to 1 ppmv. The seasonal CO<sub>2</sub> cycle is most enhanced at mid- and high northern latitudes and decreased going southward with a phase delay, but still prominent at low and mid-latitudes of the southern hemisphere where the seasonal cycle of the lower tropospheric CO<sub>2</sub> is barely observable.

The character of the seasonal CO<sub>2</sub> cycle changes south of 10°S; high and low concentrations are seen twice a year. Such variations could be explained by suppression and enhancement of southward transport of the northern hemispheric air associated with the SPCZ and the monsoon circulation in Southeast Asia. The SPCZ is usually located between 0° and 10°S on our flight routes from December to May. The lower tropospheric air in both hemispheres converges there, ascends and then returns to each hemisphere through the upper troposphere. Therefore, an inter-hemispheric air exchange is largely suppressed and the CO<sub>2</sub> concentrations are changed discontinuously, as seen in Fig. 7. During this time of the year, the upper tropospheric CO<sub>2</sub> in the southern hemisphere shows low concentrations due to the mixing of its own hemispheric

air. Slow increase of the concentration for this period may be due to horizontal diffusion of the northern hemispheric air through the SPCZ. In this connection, the northern hemispheric air is richer in CO<sub>2</sub> than the southern hemispheric air during this period except in December, and the concentration difference between both hemispheres increases gradually with time. In June, when the difference reaches a maximum, the monsoon circulation begins to occur and the SPCZ disappears, and the northern hemispheric air begins to intrude into the southern hemisphere through the upper troposphere. Since this intrusion continues until November, the CO<sub>2</sub> concentration reaches a maximum late in June or early in July and a minimum late in September, and then increases again.

Seasonal CO<sub>2</sub> cycles with almost the same amplitude and phase are observed in the upper troposphere south of 10°S. However, the seasonal CO<sub>2</sub> cycle at 7.2 km height over Sydney is quite different; maximum and minimum concentrations occur late in September and late in March, respectively, and the peak-to-peak amplitude is 1.7 ppmv.

From the above, it is suggested that southward transport of the northern hemispheric air by the monsoon circulation occurs very rapidly only through the upper troposphere, and the transported air is mixed slowly with the southern hemispheric air.

There are strong sources of various trace gases such as CO<sub>2</sub>, CH<sub>4</sub> and CFC's in the northern hemisphere, and the increase of these gases in the southern hemisphere is determined mainly by their transport from the northern hemisphere. However, this transport process is suppressed by the ITCZ and SPCZ at low latitudes, especially in the lower troposphere. Therefore, further measurements, especially with ships and aircraft, are required in the equatorial region for a better understanding of the role of these convergence zones for the transport of many trace gases from the northern hemisphere to the southern hemisphere. Knowledge from such measurements are useful for deducing spatial and temporal variations of sources and sinks of these gases.

## Figure captions

Fig. 1. Sampling routes of ship board measurements between Yokohama, Japan and Melbourne, Australia, between Tokyo, Japan and Panama and between Tokyo and Seattle, U.S.A. Also shown are those of aircraft measurements between Tokyo and Sydney, Australia and between Tokyo and Anchorage, U.S.A.

Fig. 2. Latitudinal distribution of atmospheric CO<sub>2</sub> concentration and sea surface temperature observed between Yokohama and Melbourne from late in March to early in April 1983. Symbol attached to each concentration indicates the wind direction (north; upward) and wind speed. Half and full bars correspond to 2.5 and 5 m/s, respectively

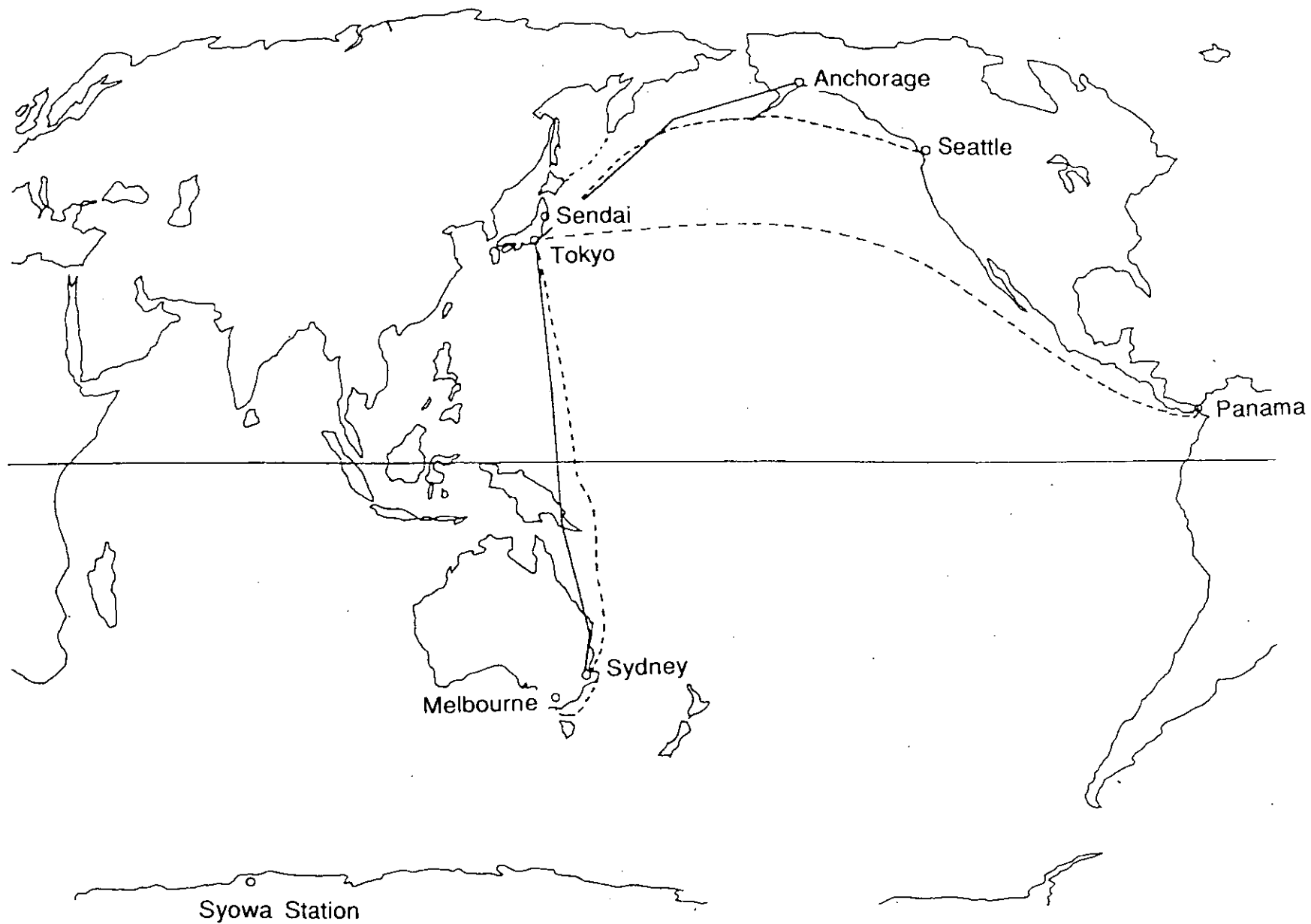
Fig. 3. Latitudinal distribution of atmospheric CH<sub>4</sub> concentration observed between Yokohama and Melbourne from early in December 1991 to early in January 1992

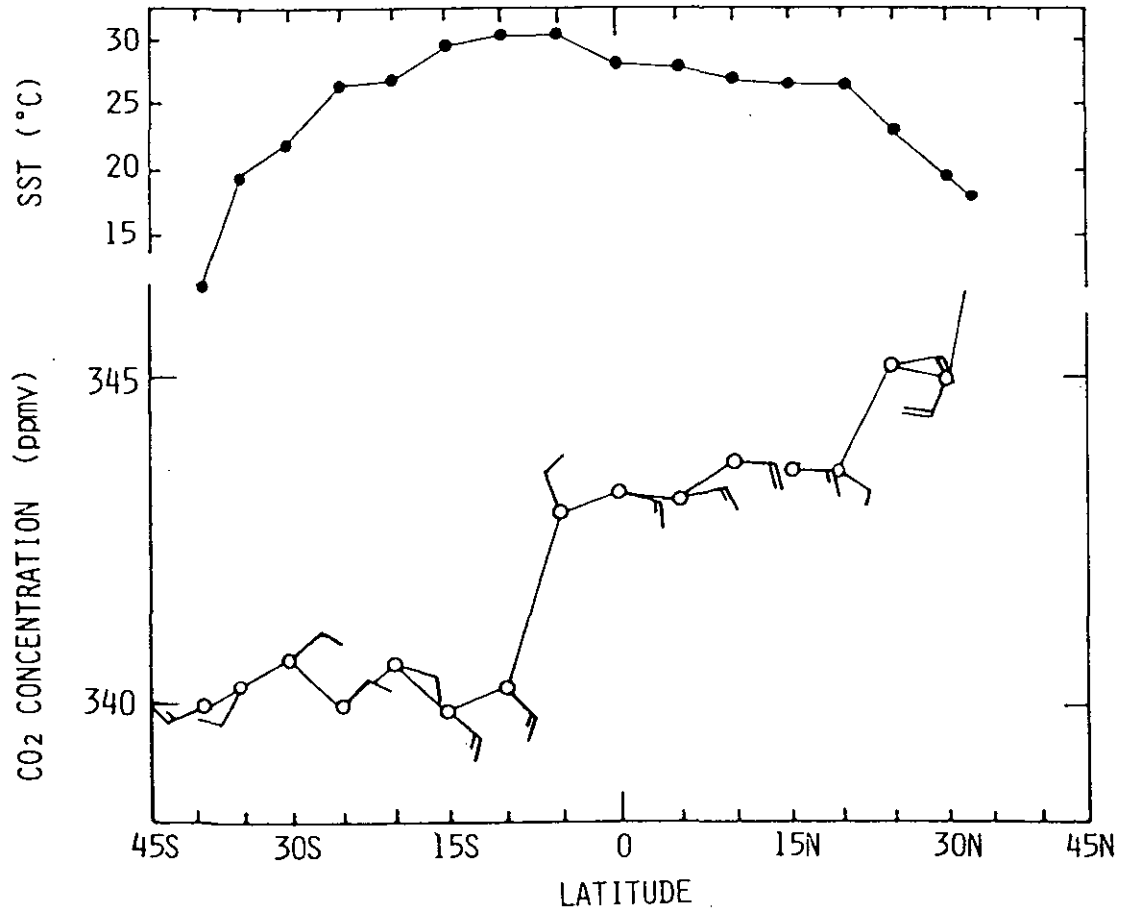
Fig. 4. Latitudinal distribution of atmospheric CO<sub>2</sub> concentration observed in the eastern part of the North Pacific Ocean for the period May 30-June 8, 1986. Bar attached to each concentration indicates the wind direction (upward; north) and wind speed

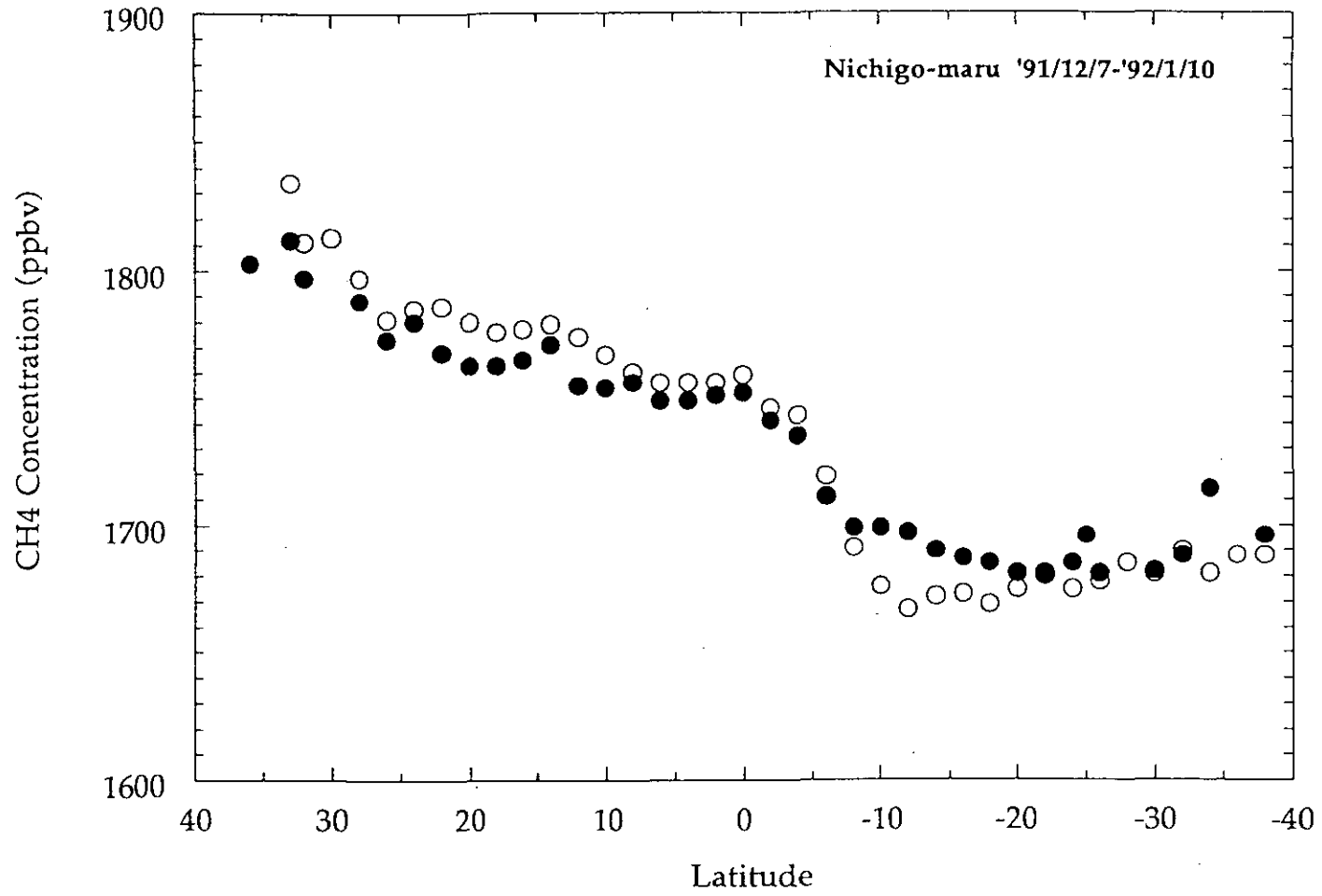
Fig. 5. Average values of yearly mean CO<sub>2</sub> concentrations of 1984 and 1985 in the lower (closed circles with solid line) and upper troposphere (open circles) and at 7.2 km height over Anchorage (closed triangle) and Sydney (open triangle). Values are represented as a deviation from the South Pole

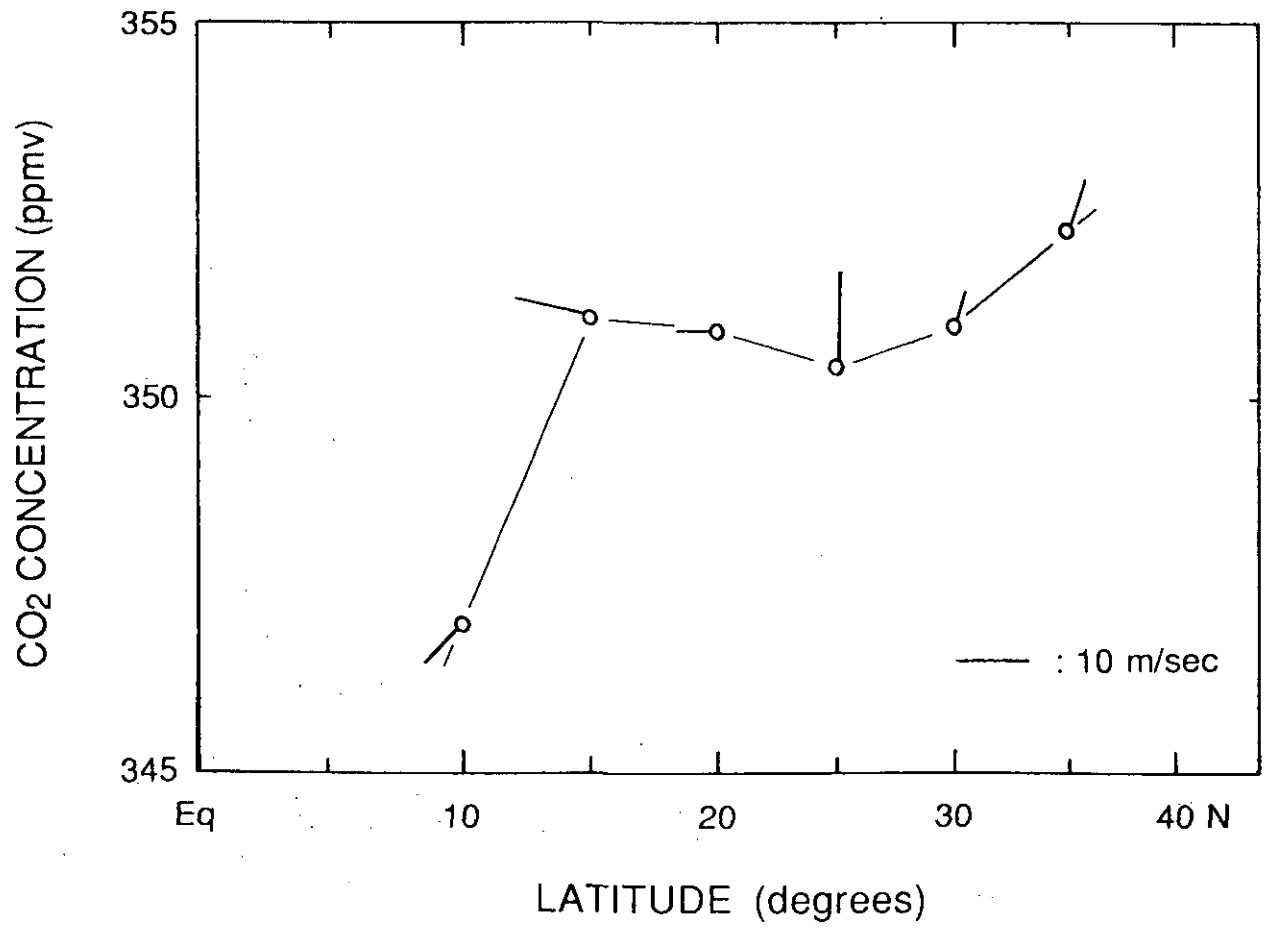
Fig. 6. Seasonal CO<sub>2</sub> cycles in the upper troposphere at respective latitudes and at 7.2 km height over Anchorage and Sydney

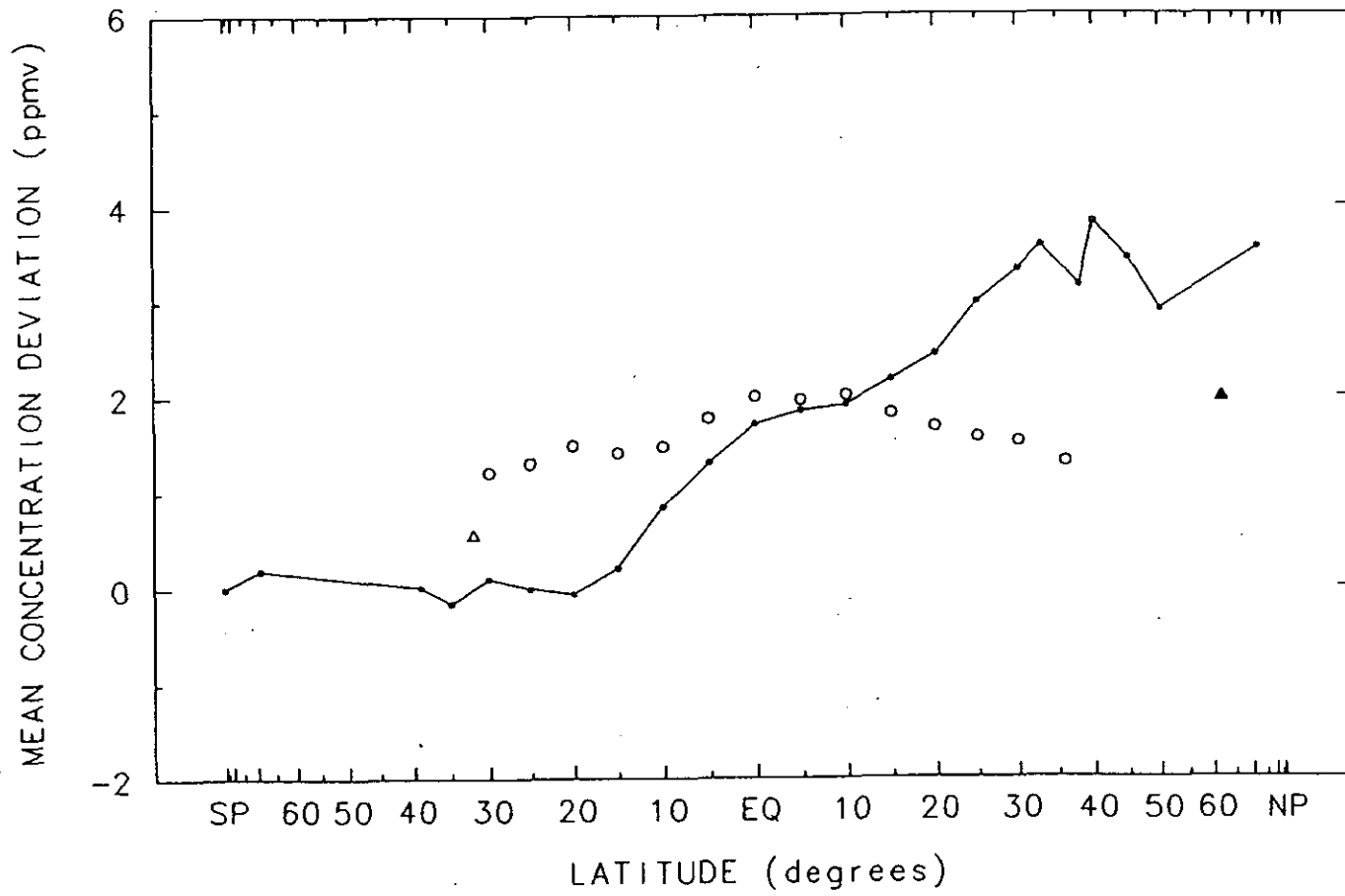
Fig. 7. Latitudinal distribution of the upper tropospheric CO<sub>2</sub> concentration between Tokyo and Sydney on February 22, 1984

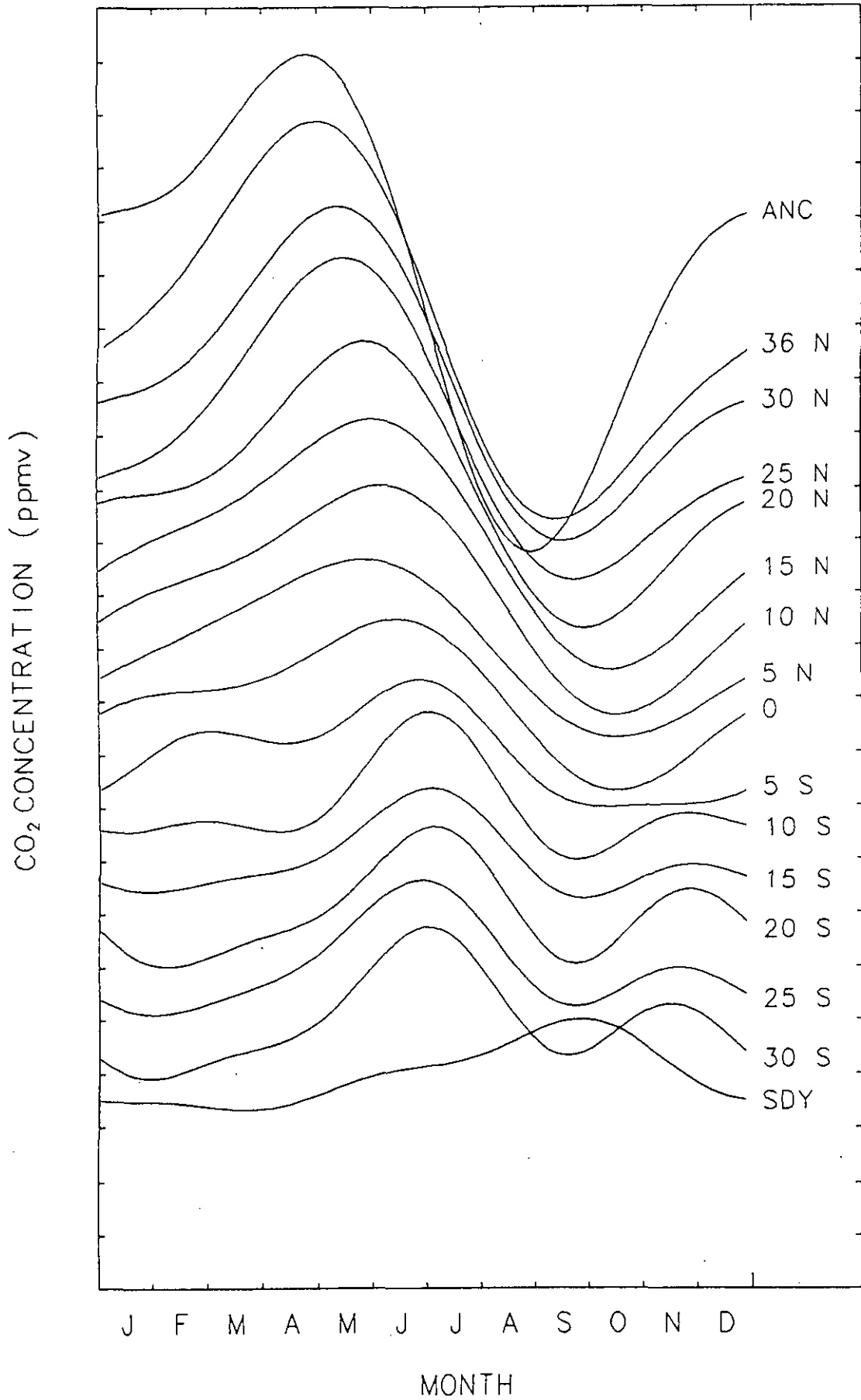


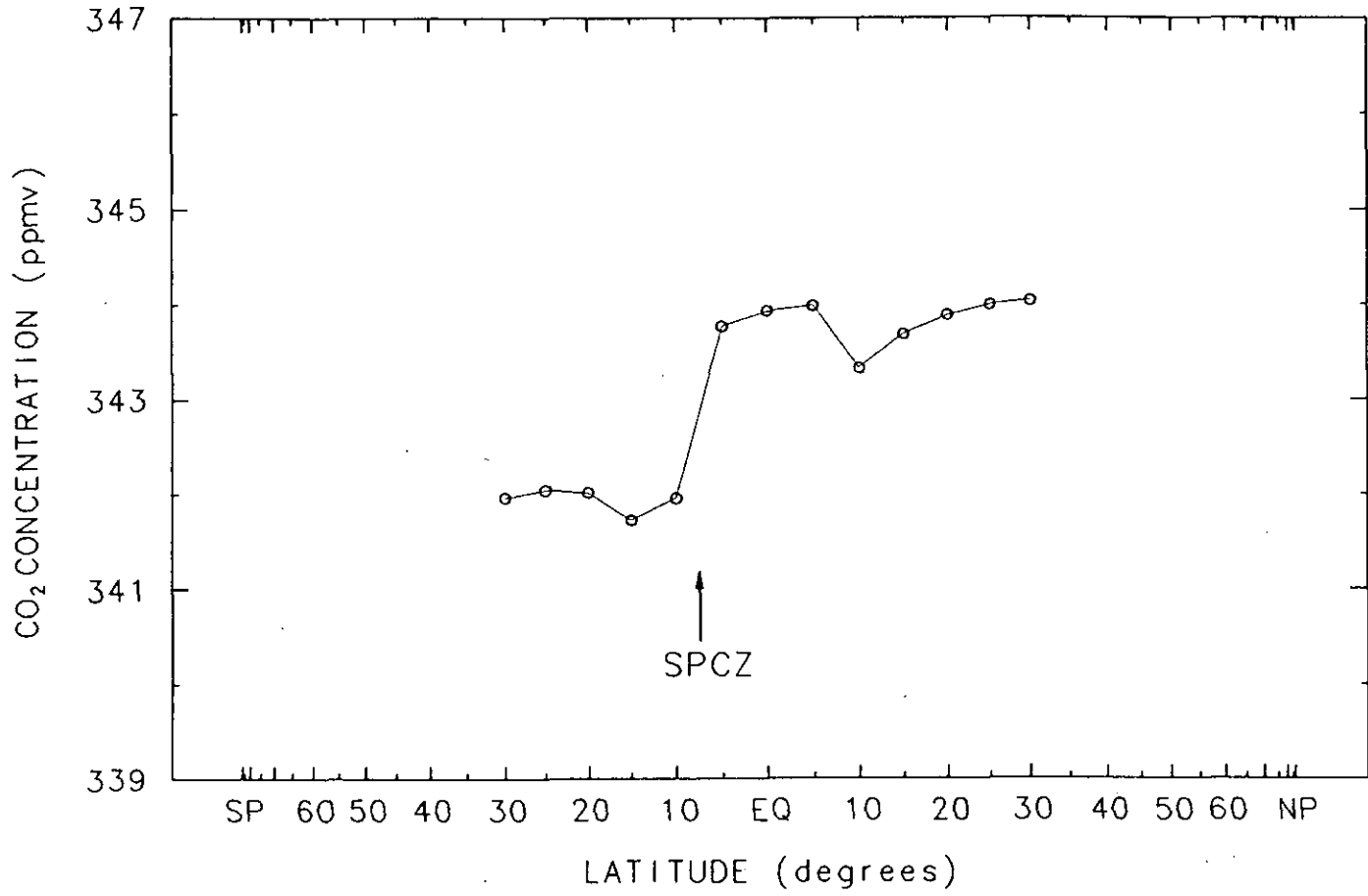












# **INSTAC**

Workshop for Trace Gas Measurement in Both Hemispheres  
March 10 - 13, 1992 at CSIRO

**Hidekazu MATSUEDA**  
Meteorological Research Institute (MRI)  
1-1, Nagamine Tsukuba-shi,  
Ibaraki-ken, 305, JAPAN

- 1) Outline of the Aircraft Observation under the Name of INSTAC.
- 2) Results of Trace Gases (Methane and Carbon Dioxide).
- 3) Post-INSTAC Projects of MRI.

# OUTLINE of INSTAC

## International Strato/Tropospheric Air Chemistry (1988 - 1990)

### 1) General purpose

To study the global distributions and behavior of trace gases in the upper atmosphere by aircraft observation to better understand the future global environmental change.

### 2) Scientific interest

2-1. To understand the meteorological transport processes of interhemispheric exchange and vertical exchange between troposphere and stratosphere.

2-2. To assess the photochemical transformation processes in the upper troposphere and lower stratosphere.

2-3. To estimate the source/sink functions from the upper atmospheric distribution.

### 3) Aircraft flight

	INSTAC-I	INSTAC-II	INSTAC-III
Date	Mar. 5-Mar 10, 1989	Feb. 20- Mar.7, 1990	Oct. 15 - Oct.22, 1990
Study area	western Pacific	western and central Pacific	western and central Pacific
Latitude	34N - 1S	65N - 65S	65N - 65S
Altitude	~ 4.5km	~ 12km	~ 12km
Aircraft	Marlin IV	Gulfstream II	Gulfstream II

### 4) Measurement

a) CH<sub>4</sub>, CO<sub>2</sub>, (C-13) (Meteorological Research Institute)

b) O<sub>3</sub>, H<sub>2</sub>O, CFCs ( Meteorological Research Institute)

c) Aerosol (Meteorological Research Institute)

d) NMHC (National Institute for Environmental Studies)

e) NO, NO<sub>y</sub> (Nagoya University)

\*This project was financially supported by the Science and Technology Agency of Japan.

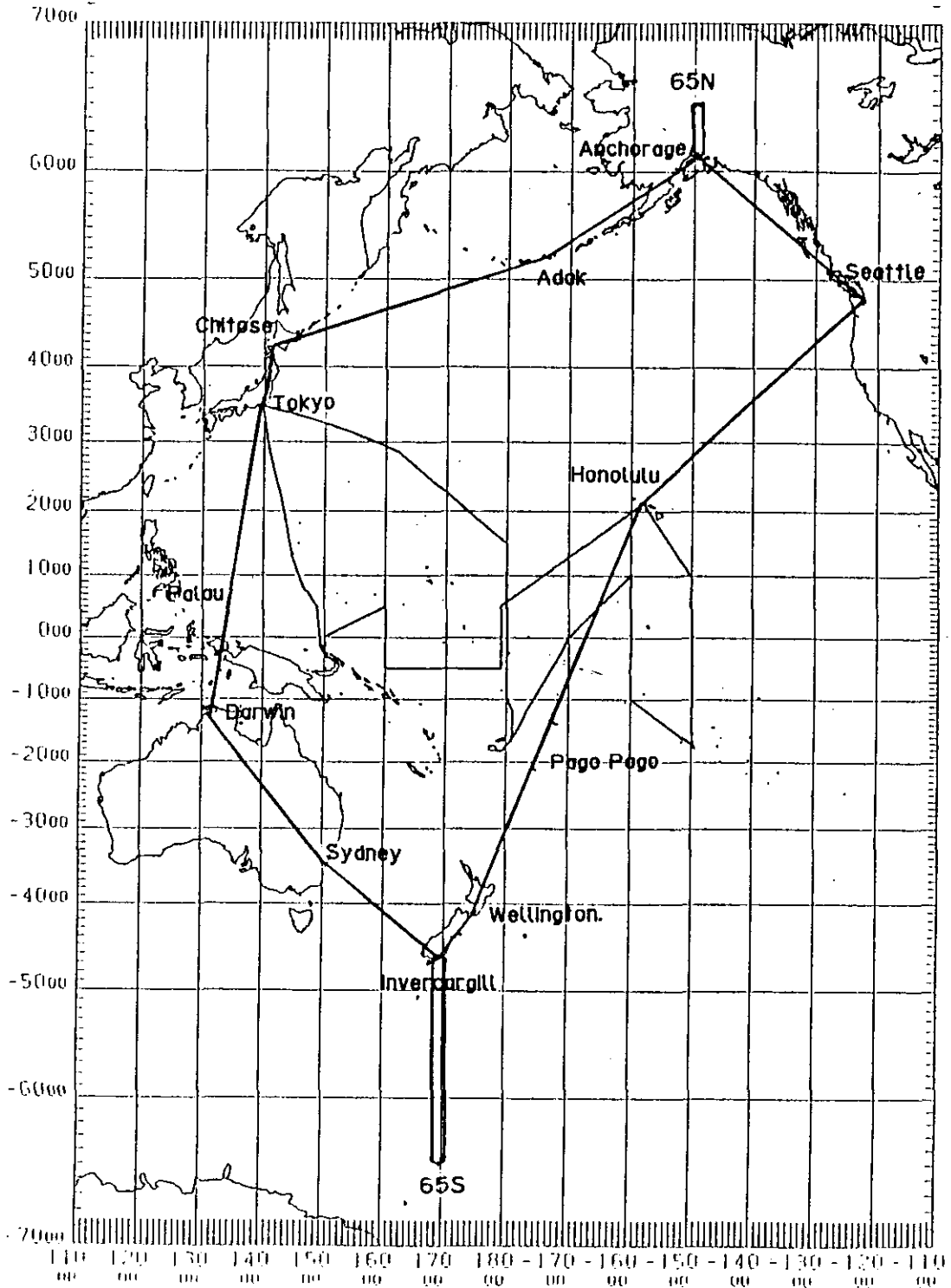
12 Km

INSTAC-II (Feb.20-Mar.7, 1990)

INSTAC-III (Oct.15-Oct.22, 1990)

0 Km

KH9009 (Sep.-Dec., 1990)



## Sampling and Analysis

### (A) Sampling

1) Inlet

Stainless steel inlet mounted ahead of engine to avoid the contamination from the aircraft

2) Sample bottle

Stainless steel bottles with internal volume of 3 or 5 liters

3) Pump

Metal bellows pump (MB158 and MB41)

4) Sample pressure

About 1.6 atmospheres

### (B) Analysis

	Methane	Carbon dioxide
Method	GC-FID	NDIR analyzer
Analytical error	~ ±0.2% (1σ)	~ ±0.02ppm (1σ)
Standard gas scale	Nippon Sanso Company, Japan	Nippon Sanso Company, Japan

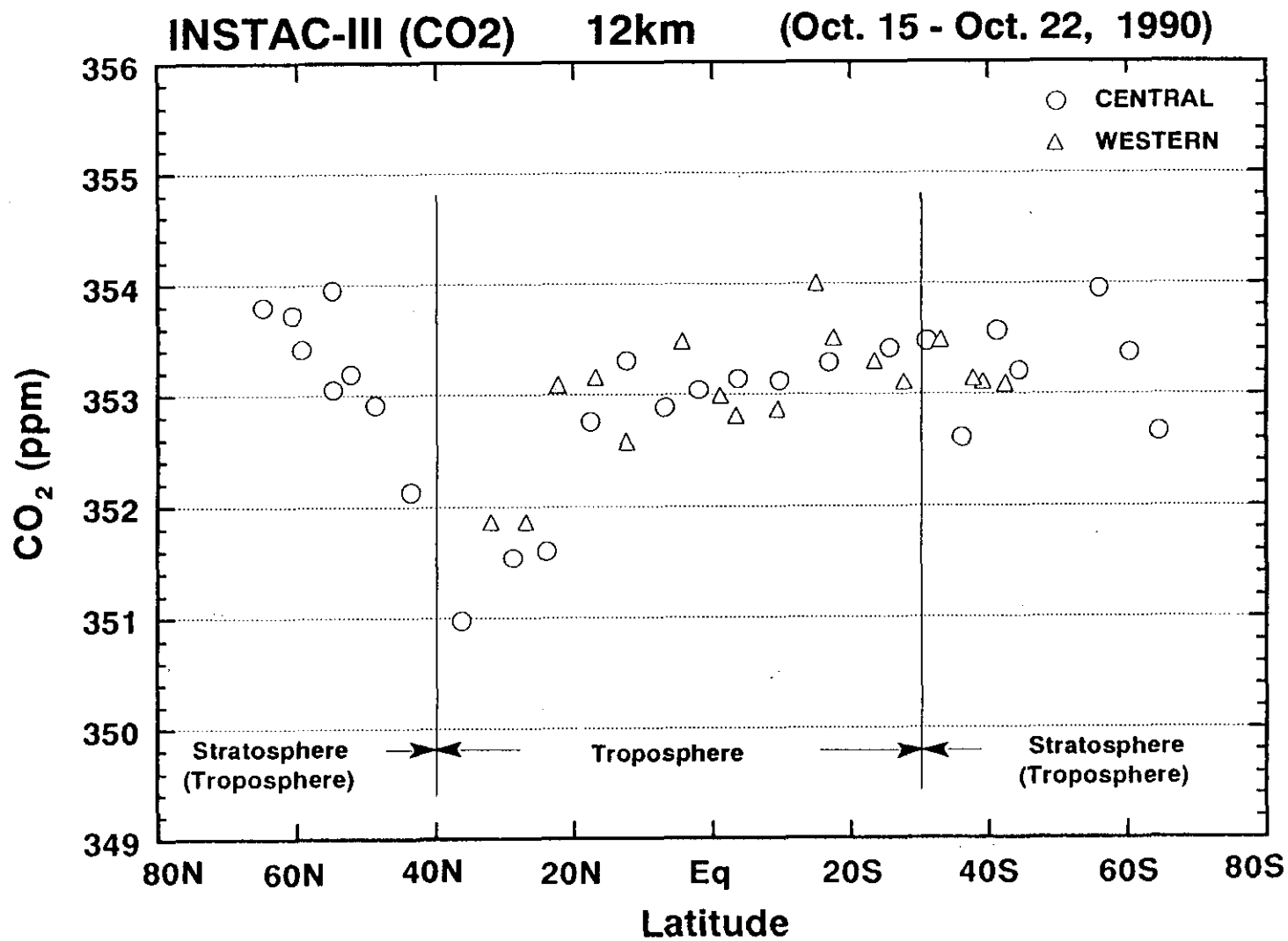
### (C) Storage test

1) Methane

No drift.

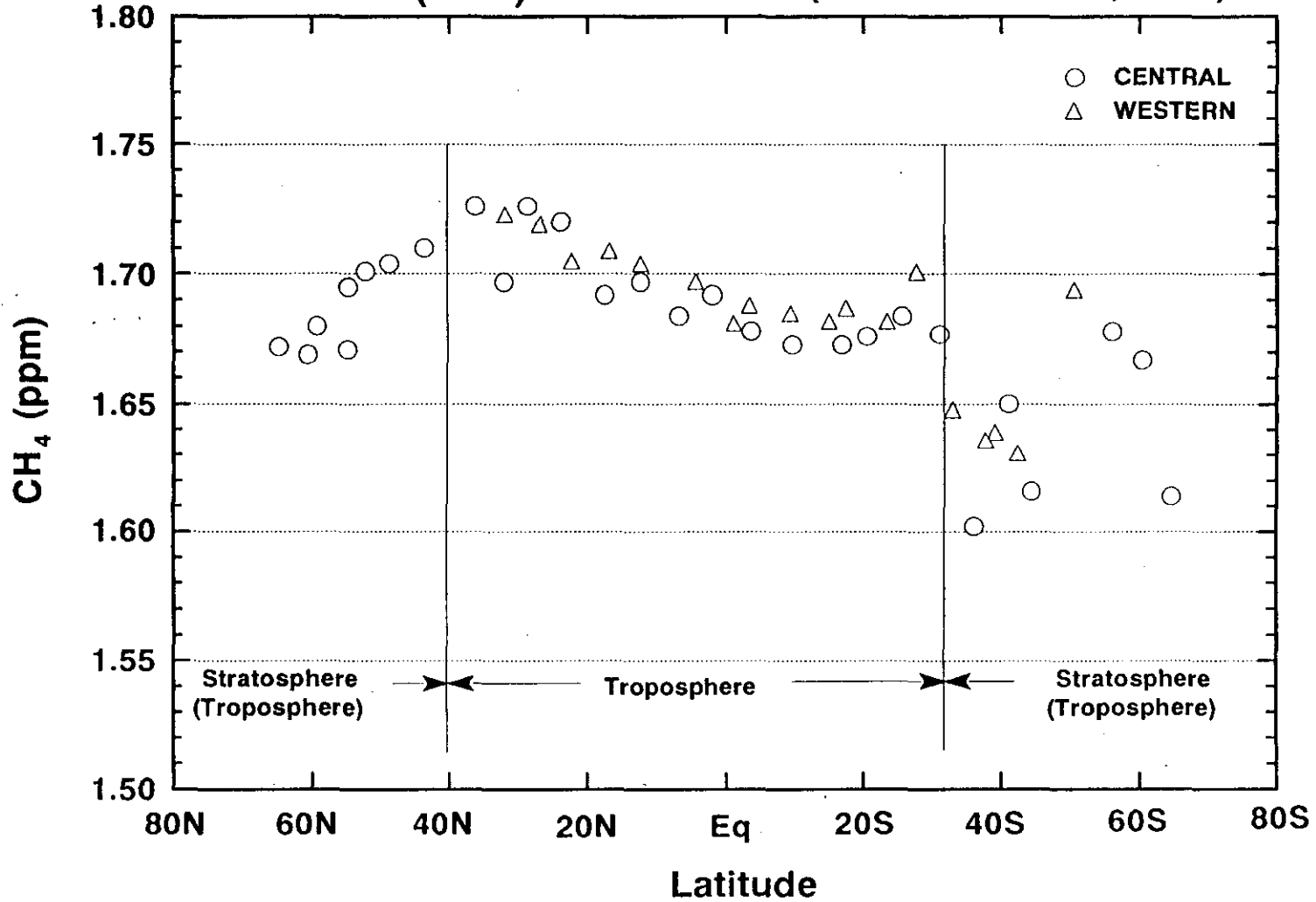
2) Carbon dioxide

Small drift (~0.005ppm/day)

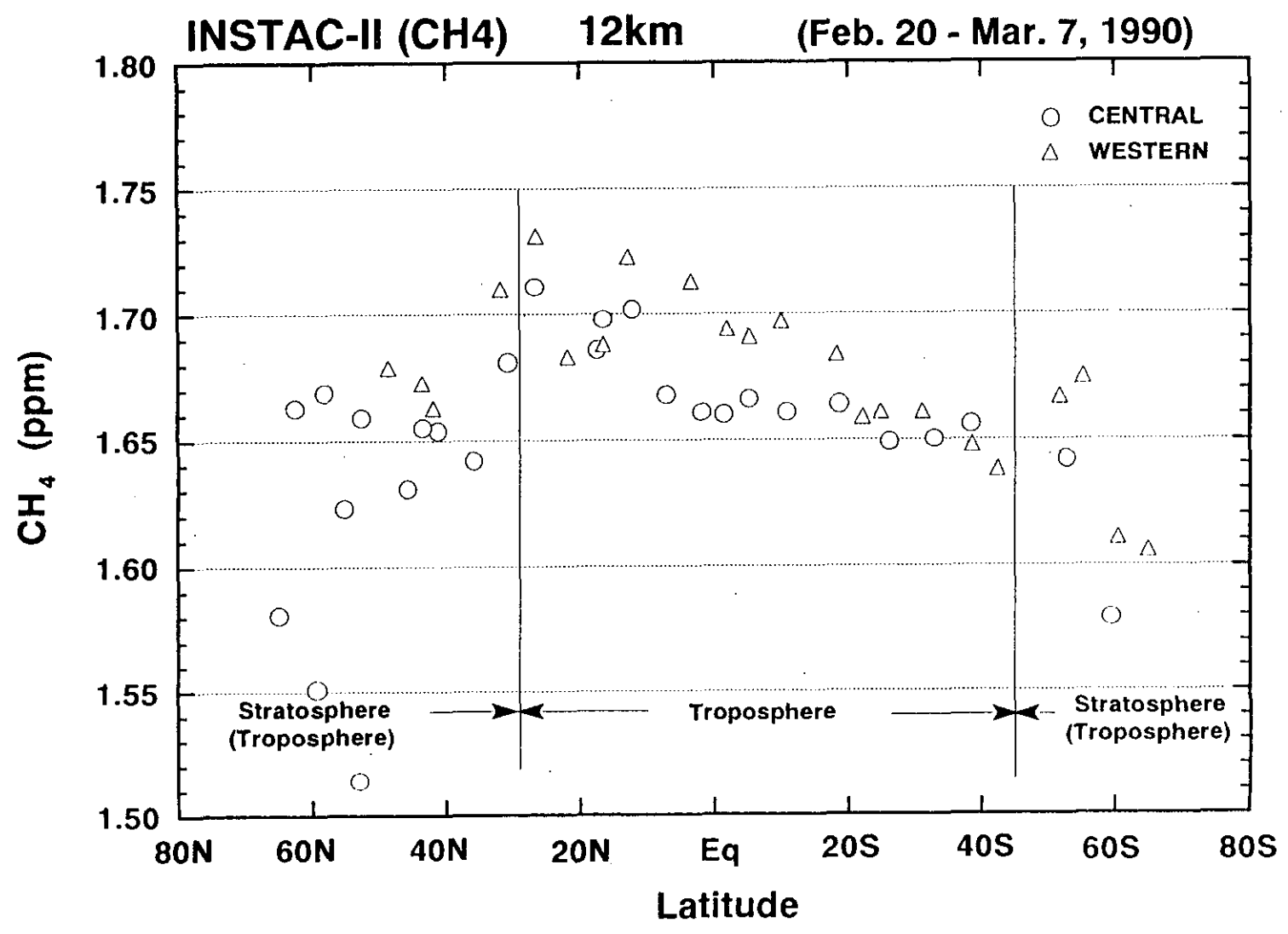


*Matsueda et al. (unpublished) Not for citation*

**INSTAC-III (CH<sub>4</sub>) 12km (Oct. 15 - Oct. 22, 1990)**



Matsueda et al. (unpublished) Not for citation



## Post-INSTAC Project of MRI

### 1) General Purpose

Regular observation in the upper, middle and lower atmosphere over the western Pacific using aircrafts and ships to clarify the seasonal and interannual variabilities of vertical distributions of trace gases.

### 2) Outline of Post-INSTAC Projects of MRI

Altitude	Upper Troposphere ~ 12km	Middle Troposphere ~ 5km	Lower Troposphere Surface
Aircraft or Ship	Commercial Passenger Aircraft (JAL)	Scientific Research Aircraft	Trading Vessel
Study Area	Western Pacific from Japan to Australia	Western Pacific from Japan to Australia	Western Pacific from Japan to Australia
Sampling	Monthly	1 or 2 times per year	Bimonthly
Project	On Going	On Going	Planning

Aerosol Microphysical Measurements  
within the WMO GAW Environment.

J. L. Gras

CSIRO Division of Atmospheric  
Research

Workshop for Trace Gas Measurement  
in Both Hemispheres  
Melbourne, March 1992.

## TALK OUTLINE

- Why microphysics, CN, CCN, aerosol optics?
- The WMO GAW program
- Cape Grim - Southern Ocean program

# CLIMATE ROLES OF ATMOSPHERIC AEROSOL

## 1/ DIRECT RADIATIVE EFFECTS

Charlson et al. (1991), N.H. Sulfate  
around  $-1.1 \text{ Wm}^{-2}$

## 2/ INDIRECT CLOUD ALBEDO RADIATIVE EFFECTS

Twomey (1984),

Charlson et al. (1987), +30% CCN  $\rightarrow -1.8 \text{ Wm}^{-2}$

Wigley (1989) N. H. +20%  $\rightarrow -1 \text{ Wm}^{-2}$

## 3/ ROLE OF CLOUD IN HYDROLOGICAL CYCLE

CN an indicator of the dynamics between  
production of aerosol from reactive gases and loss  
processes.

# **Proposed WMO GAW Aerosol Measurement Program**

## **Regional and Baseline stations**

- 1/ Optical depth (multi-wavelength) [A]
- 2/ CN concentration
- 3/ Sub micrometre aerosol mass/composition [B]  
Super micrometre aerosol mass/composition

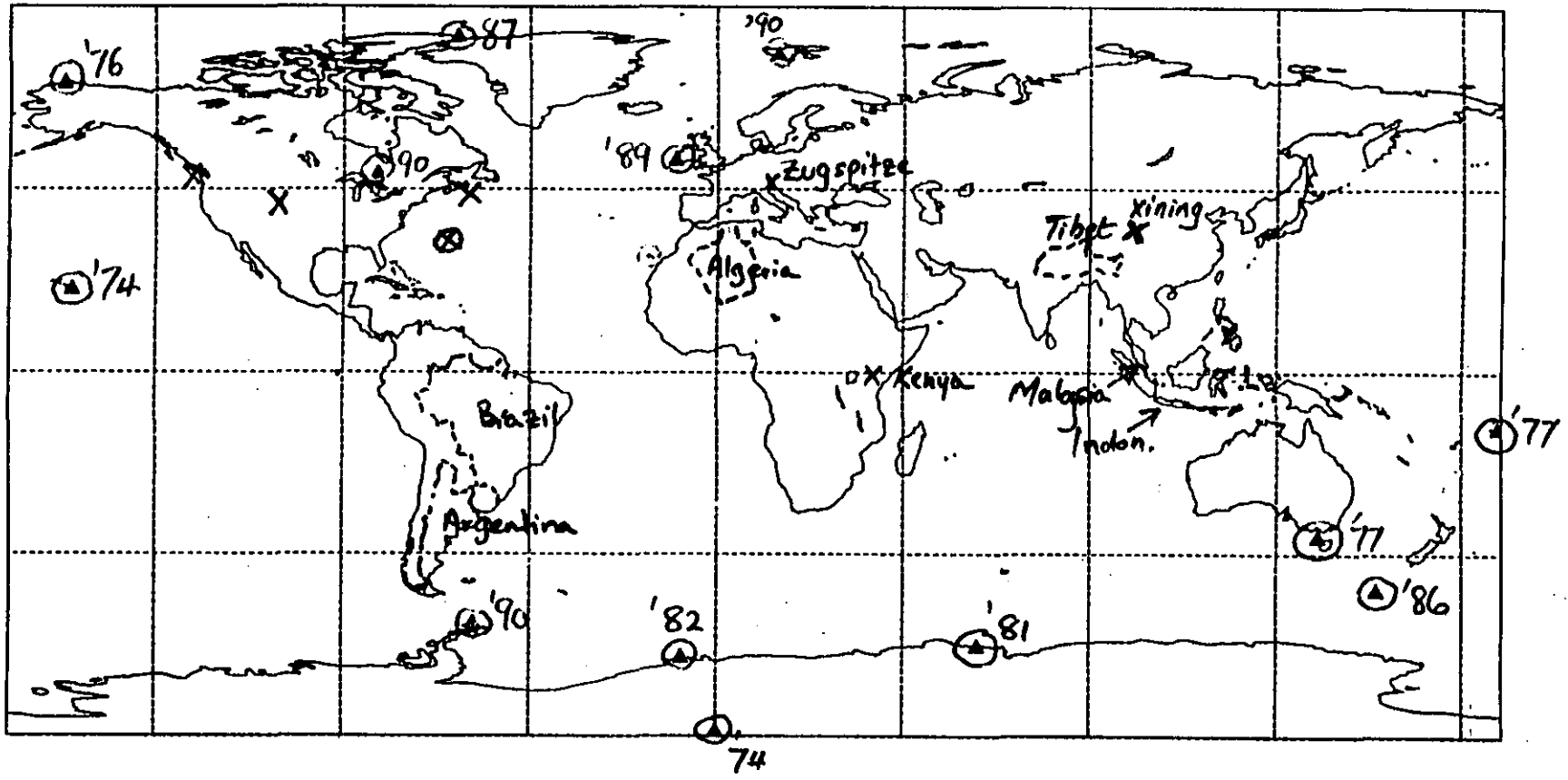
## **Baseline stations**

- 4/ Aerosol scattering coefficient (multi-wavelength) [C]  
Aerosol absorption coefficient (same wavelengths)
- 5/ CCN concentration [C]
- 6/ Backscatter coefficient (LIDAR), some sites [D]
- 7/ Diffuse, total radiation [E]
- 8/ Aerosol size distribution,  $n(r)$ , some sites [E]

## **Priorities [A-E]**

CN

⊙ ACTIVE      X PLANNED  
                  X POSSIBLE



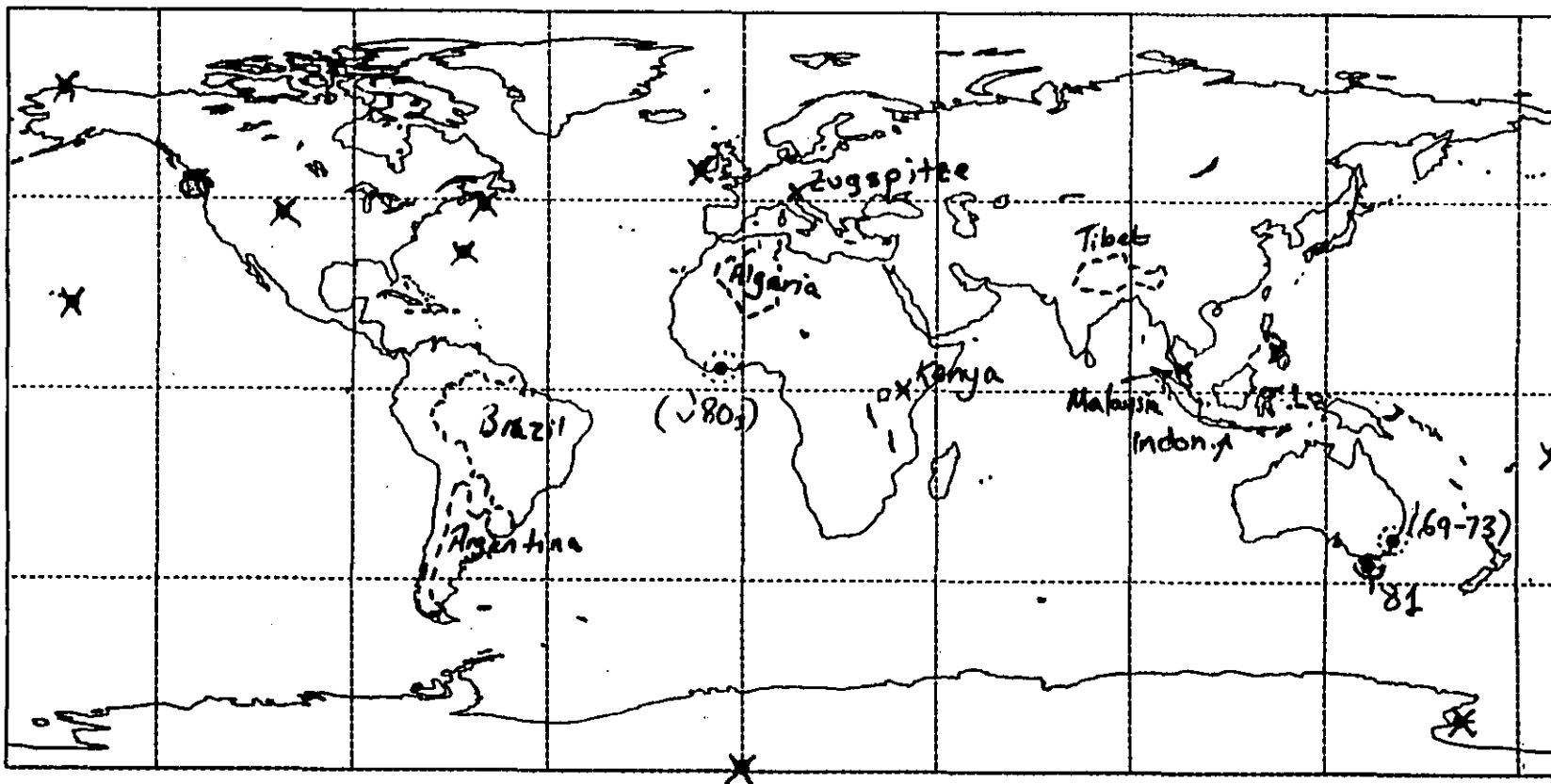
CCN

⊙ ACTIVE

⊙ PAST

X PLANNED

X POSSIBLE



## **Timescale for CCN program startup.**

**existing:** Cape Grim (1981)

(prior: Robertson, Aust. 1969-1973)

U. of Wa., Cheeka Pk., 1991

**planned:**

UCG.: Mace Head, objective: mid 1992

NOAA CMDL: (a) Cheeka Pk. (with U. of Wa.), Sable Isl., Bermuda, Elk Mtn. Wyoming

(b) Barrow, Mauna Loa, Samoa, South Pole.,

objective: initial implementation 1992, then progressive.

NZ Met.: Scott Base, objective 1992

WMO: Argentina, Brazil, Algeria, Tibet,

aerosol/CCN objective: late 1993

Zugspitze-Wang 1994?

Kenya, Malaysia, Indonesia, minimum aerosol program,

objective: by 1994.

## Southern Ocean - Antarctic Aerosol Programs

### **Cape Grim (40.7 °S, 144.7 °E)**

1976 Hivol: MSA, SALT, (nss SO<sub>4</sub> ?)

1977 CN Auto Nolan-Pollak

1981 CCN Static, thermal gradient

1983 CN diffusion battery

1984 CN TSI 3020

1985 Hivol PM10, MSA, nss SO<sub>4</sub>

1989 DMS, nss SO<sub>4</sub>

1990 Size distn. 0.05-1.5 μm radius

1990 Elemental C

1990 SO<sub>2</sub>

### **Mawson (67.6 °S, 62.9 °E)**

1981 CN Auto Nolan-Pollak

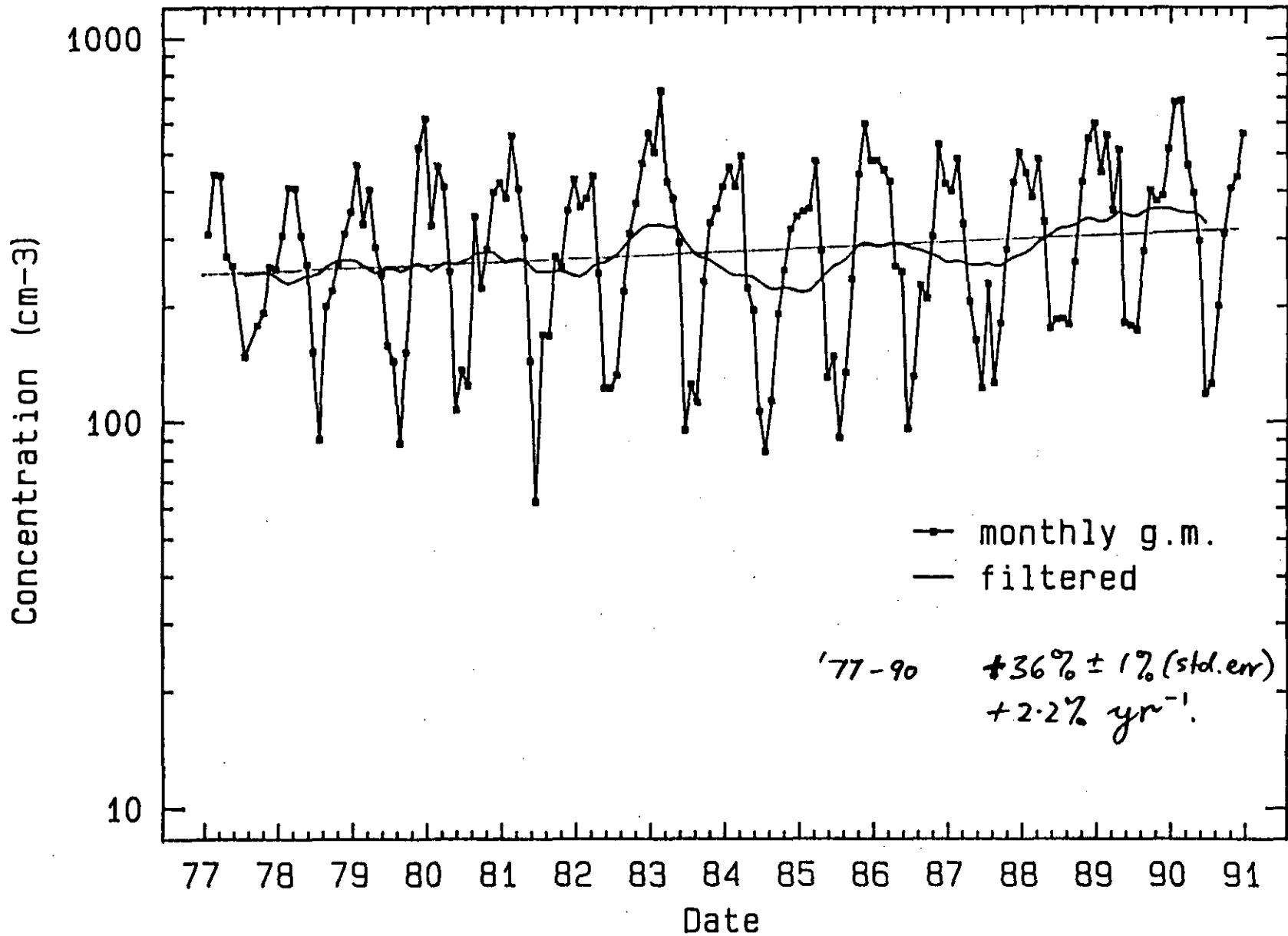
1982 CN diffusion battery

1987 Hivol (Miami) MSA, nss SO<sub>4</sub>, NO<sub>3</sub>

1989 CSIRO MSA, nss SO<sub>4</sub>, NO<sub>3</sub>

1992 DMS, SO<sub>2</sub>

Cape Grim CN concentration 1977-1990



## SUMMARY

\* MAJOR reason for aerosol program are direct and indirect radiative effects and hydrological cycle.

\* WMO GAW aerosol program - 8 components for Baseline programs. Covers aerosol composition, direct and indirect climate forcing.

\* GLOBAL coverage by GAW from aerosol point of view is fairly sparse, (particularly CCN).

\* Cape Grim aerosol program started 1976, main emphasis S cycle, indirect climate effect. More emphasis on aerosol radiative properties in future.